# UNIVERSITY OF PARDUBICE

FACULTY OF CHEMICAL TECHNOLOGY

Institute of Environmental and Chemical Engineering

**Edwin Wallace**


# The use of nanofiltration for separation of heavy metals from wastewater

*Doctoral Dissertation*


Pardubice 2020

Study program: **Chemical and Process Engineering**

Study field: **Environmental Engineering**

Author: **Edwin Wallace**

Supervisor: **prof. Ing. Petr Mikulášek, CSc.**

Year of defence: 2020

## References

WALLACE, Edwin. *The use of nanofiltration for separation of heavy metals from wastewater*. Pardubice, 2020. 138 pages. Dissertation thesis (PhD.). University of Pardubice, Faculty of Chemical Technology, Institute of Environmental and Chemical Engineering. Supervisor Prof. Ing. Petr Mikulášek, CSc.

## Abstract

The aim of this research is to investigate the performance of two commercially available thin–film composite polyamide NF membranes (AFC 30 and AFC 80) for separating toxic heavy metals from wastewater. Structural parameters and charged surface properties of the membranes were estimated. Experiments with neutral aqueous solutions in conjunction with two independent pore models (Donnan Steric Pore and Steric Hindrance Pore model) were performed at various process conditions. The fixed charge density (ΦX) on the membrane surfaces were determined from different concentrations of sodium chloride (NaCl) experiment by using the Spiegler–Kedem model together with Teorell–Meyer–Sievers model (TMS). The influence of the operating conditions such as transmembrane pressure, feed concentration, cross–flow velocity, pH and effect of composition solution on heavy metals were studied. The operating parameters have been used to find optimum conditions of the two tested commercially available nanofiltration membranes for the removal of heavy metals from wastewater. Heavy metals rejection was modelled using Spiegler–Kedem model and Steric Hindrance Pore model.

## Abstrakt

Tato práce se zabývá uplatněním dvou komerčně dostupných tenkovrstvých kompozitních polyamidových NF membrán (AFC 30 a AFC 80) pro odstraňování toxických těžkých kovů z vod. Byly zjišťovány strukturní parametry a povrchový náboj. Byly provedeny experimenty s neutrálními látkami za různých podmínek společně se dvěma modely popisující porézní strukturu (Donnanův sterický model a sterický model). Hustota fixovaného náboje na povrchu membrány (ΦX) byla zjištěna na základě experimentů s chloridem sodným (NaCl) a pomocí modelu Spiegler–Kedemové společně s Teorell–Meyer–Sievers modelem (TMS). Byl testován vliv operačních parametrů jako tlakový rozdíl nad a pod membránou, koncentrace nástřiku, rychlost proudění nástřiku, pH a složení roztoku těžkých kovů. Testování bylo prováděno za účelem získání optimálních podmínek pro separaci těžkých kovů pomocí dvou komerčně dostupných NF membrán z odpadní vody. Rejekce těžkých kovů byly modelovány na základě modelu Spiegler–Kedemové a sterického modelu.

## Keywords

Heavy metals, rejection, nanofiltration, polyamide membrane, modelling

## Klíčová slova

Těžké kovy, rejekce, nanofiltrace, polyamidová membrána, modelování

# Table of Contents

## List of Figures



## List of Tables

## Introduction

During the past decades, about 50–90 % of capital investments in the chemical industry are related to separation processes of heavy metals from wastewater. Yet, several concerns have been raised on heavy metals due to its recalcitrance and persistence into the environment which poses a threat to humans and aquatic life. It has also become crucial that regulatory measures need to be set up on the effluent limit globally as the industries realize its potential environmental impacts (Geens et al., 2007; Zhao et al., 2016). Heavy metals are defined as a group of elements having atomic weights between 63.5 and 200.6 (O' Connell et al. 2008; Srivastava and Majumder, 2008). According to Tchounwou et al., 2012, heavy metals refers to any metallic element that has a relatively high density and is toxic or poisonous even at low concentrations. Heavy metals were further explained as a general collective term, which applies to a group of metals and metalloids with atomic density greater than 4000 $kg.m^{-3}$. Heavy metal is highly toxic, non-biodegradable and has the tendency to accumulate in living organism. Additionally, heavy metals cannot be degraded or destroyed. Toxic heavy metals of critical concerns found in wastewater treatment are cadmium (Cd), chromium (Cr), nickel (Ni), copper (Cu), lead (Pb), arsenic (As), cobalt (Co), mercury (Hg) and zinc (Zn). Heavy metals are usually found in wastewater from fuel industry, petroleum refining, mining, textile industry, fertilizer plants, battery manufacturing, paper industries, photographic process industry, automotive and electroplating (Gherasim and Mikulášek, 2014). Furthermore, although heavy metals are naturally occurring elements that are found throughout the earth's crust, most environmental contamination and human exposure result from anthropogenic activities such as mining and smelting operations, industrial production and use, and domestic and agricultural use of metals and metal-containing compounds. Heavy metals toxicity depends on several factors including the dose, route of exposure, and chemical species, as well as the age, gender, genetics, and nutritional status of exposed individuals. At least 20 metals are toxic, and almost half of these metals enter the environment which poses a threat to aquatic life and human beings (Tchounwou et al., 2012).

Separation of heavy metals from wastewater is paramount in this our $21^{st}$ century due to its recalcitrance, persistence, and tendency to build-up in living organism. In addition, heavy metals cannot be degraded or destroyed in the environment without proper separation. (Fu and Wang, 2011; Gherasim et al., 2015; Murthy and Chaudhari, 2008). Numerous approaches have been employed for the development of cheaper and more effective technologies, both to decrease the amount of wastewater produced and improve the quality of separation processes involved (Barakat, 2011). Diverse conventional technique has been carried out over the years to remove heavy metals from industrial effluents. These methods include chemical precipitation, solvent extraction, adsorption, ion exchange, coagulation/flocculation, electrochemical treatment, and floatation (Fu and Wang, 2011). Conversely, conventional separation processes involve high operational cost due to chemical consumption, high initial cost, and increased volume of sludge generated. Furthermore, these methods are slow and laborious due to collection of disposal sludge or addition of high level of chemicals. These chemicals have failed to meet regulation level set up by individual countries in terms of technical, economic, and environmental reasons (Malik et al., 2012).

Membrane process has been determined as feasible and promising option due to its high efficiency, no phase change, convenient operation, and many advantages over the conventional methods (Wei et al., 2013). For the removal of heavy metals from aqueous solution, membrane processes such as liquid membranes and pressure driven processes like nanofiltration, reverse osmosis and hybrid processes have been used (Gherasim and Mikulášek, 2014). In this research, the pressure driven processes will be discussed specifically nanofiltration.

## Theoretical background

### 1. Pressure driven membrane processes

A pressure driven membrane process are subset of membrane separation processes which include microfiltration (MF), ultrafiltration (UF), nanofiltration (NF), and reverse osmosis (RO) (Baker, 2004). Pressure driven membrane processes can be classified by several criteria such as the characteristics of the membrane (pore size), size and charge of the retained particles or molecules, and pressure exerted on the membrane. Particles and dissolved components are (partially) retained based on properties such as size, shape, and charge. These membrane processes use the pressure difference between the feed and permeate side as the driving force to transport the solvent (usually water) through the membrane (Van der Bruggen et al., 2003). The driving force in pressure driven membrane separation, is of course, the pressure, or the pressure difference between the upstream and the downstream of the membrane, or between the feed and the permeate. This pressure difference is known as transmembrane pressure. Fig. 1 gives a clear overview of classification on the applicability of different membrane separation processes based on pore size, pressure and their application (Hung et al., 2017).

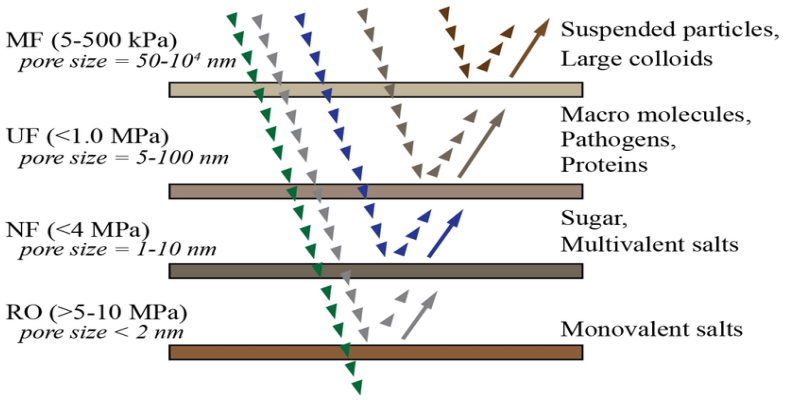


Fig. 1. The ranges of pore sizes, applied transmembrane pressure, and applications of pressure driven membrane processes (Hung et al., 2017).

Among all this pressure driven processes, NF membrane has received greater attention and made tremendous progress since its introduction in the 1980's (Mohammad et al., 2015). NF membranes have been useful in many applications particularly in wastewater treatment as well as drinking water and process water production. The interest in the use of NF membrane can be explained by a combination of (i) growing demand for water with high quality, (ii) growing attention to reuse water due to rapid population globally (iii) better dependability and integrity of the membranes (iv) lower

cost of membranes due to improved use and (v) more stringent water standards (Van der Bruggen et al., 2008). Hence, it is significant to analyse proper separation process such as nanofiltration which can be useful to remove heavy metals from wastewater. In general, the key factor for removal of heavy metal from wastewater depends on the characteristics of wastewater, operational cost, applicability, and process simplicity. In addition, the separation process should be suitable, appropriate, and meet the environmental–based treatment standard level set by the established country (Zhao et al., 2016).

## 2. Concentration polarization phenomena

By analysing the solute concentration in the feed side ($c_f$) and permeate ($c_p$), the observed rejection can be calculated from the following equation:

$$R_o = 1 - \frac{c_p}{c_f} \tag{1}$$

The real (intrinsic) rejection was derived from the film model when taking effect of the concentration polarization and is as follows (Mulder, 1997):

$$R = 1 - \frac{c_p}{c_m} = \frac{R_o exp\left(\frac{J}{k}\right)}{1 - R_o\left[1 - exp\left(\frac{J}{k}\right)\right]} \tag{2}$$

where $c_m$ is the concentration of solute in the feed solution at the membrane surface (vicinity), $J$ is the permeate volume flux and $k$ is the mass transfer coefficient in the polarization layer which can be calculated from the well–known Sherwood relationship with Deissler correlation (Mulder, 1997).

## 3. Characterization of a membrane by using neutral solutes rejection

### 3.1 Donnan Steric Partitioning (DSP) model

Bowen et al. (1997) originally developed the Donnan steric partitioning model based on the extended Nernst Planck equation. Pore are modelled as bundles of cylindrical pore radius $r_p$ and length $\Delta x$ (with $\Delta x \gg r_p$) or as a bundle of slits with length and the half width. The structural parameters which are the effective pore size ($r_p$), as well as membrane thickness to porosity ratio ($\Delta x/A_k$), were estimated through independent experiments with neutral solutes rejections. In NF membrane, the rejection of neutral solutes can only be determined by a steric mechanism (size–based exclusion). The pore radius can be found by fitting the rejection using the following equation (Bowen et al., 1998; Cavaco Morãoa et al., 2008):

$$R = 1 - \frac{c_p}{c_m} = 1 - \frac{\phi_i K_{i,c}}{1 - [(1 - \phi_i K_{i,c}) exp(-Pe)]} \tag{3}$$

where $\phi_i$ is steric partitioning coefficient of the solute $i$, $K_{i,c}$ and $K_{i,d}$ are the hindrance factors for convection and diffusion.
The Peclet number ($Pe$) is defined by the expression:

$$Pe = \frac{K_{i,c} J}{K_{i,d} D_{i,\infty}} \frac{\Delta x}{A_k} \tag{4}$$

where $A_k$ is the membrane porosity and $\Delta x$ is the effective membrane thickness.
The hindrance factors for convention and diffusion (slit–like pores) can be evaluated by the following equations found in a literature by Dechadilok and Deen (2006).
The salt diffusion coefficient ($D$) was computed based on the diffusion coefficient ($D_+$, $D_-$) and valences ($z_+$, $z_-$) of the individual ions (cation and anions) by using the following equation (Vanýsek, 2005):

$$D = \frac{(z_+ - z_-)D_+D_-}{z_+D_+ - z_-D_-} \tag{5}$$

### 3.2 Spiegler–Kedem model

The Spiegler–Kedem model makes use of irreversible thermodynamics (IT) for describing the transport of single solute and solvent in both NF and RO. This model describes the membrane as an empirical 'black box' by neglecting the porosity of the membrane as well as detail transport mechanism (Agboola et al., 2015). The solvent and solute transport is described by a sum of convective (due to the pressure gradient) and diffusive (due to the concentration difference existing at the membrane sides) fluxes. The three transport coefficients which satisfy the Spiegler–Kedem model are the reflection coefficient (σ), the solute permeability ($P$), and the water permeability ($L_p$) (Hidalgo et al., 2013). The equations can be found in the article by Gherasim et al., 2013. From the Spiegler–Kedem model, σ and $P$ can be determined by fitted these values with the rejection (Spiegler and Kedem, 1966).

### 3.3 Steric Hindrance Pore (SHP) model

Nakao and Kimura (1982) proposed the steric hindrance pore (SHP) model that was modified from the pore model. Therefore, the pore radius and membrane porosity ratio can be calculated from the following Eqs. (6) and (7) as σ and $P$ are already known (from Spiegler–Kedem model):

$$\sigma = 1 - (1 + \frac{16}{9}\,\lambda^2)\,(1-\lambda)^2\,[2 - (1-\lambda)^2] \tag{6}$$

$$P = D_s\,(1-\lambda)^2\,(A_k\,/\Delta x) \tag{7}$$

### 3.4 Teorell–Meyer–Sievers model (TMS)

The Teorell–Meyer–Sievers (TSM) model has been used successfully in many types of research works. It describes the transport characteristics of solutes through the NF membrane by the electrical properties (Gherasim et al., 2014; Hoffer and Kedem, 1967). It explains the transport of charged solutes through the membranes is by only the electrostatic effects. The TMS assumes uniform distribution of fixed charges in a membrane and used to investigate the membrane potential, the effective fixed charged density, and salt rejection of a charged membrane (Wang et al., 1995). In addition, the model is widely used to determine the electrical properties (effective fixed charge density of the membrane $\Phi X$). Since is a salt solution of a 1–1 type electrolyte and a negative charged NF membrane, the TMS model equations which involve reflection coefficient (σ) and solute permeability ($P$) are given the following equation (Wang et al., 1995):

$$\sigma = 1 - \frac{2}{(2\alpha - 1)\xi + (\xi^2 + 4)^{1/2}} \quad (8)$$

$$P = D_s(1 - \sigma)\frac{A_k}{\Delta x} \quad (9)$$

where $\xi$ is the parameter which expresses the electrostatic effects and is defined as the ratio of the fixed charge density of the membrane ($X$) to the concentration of the 1-1 electrolyte ($c$). The TMS model in Eq. (7) can be simplified when the transport number of cations in the free solution (α) was calculated with constant value of 0.3954. When this value is inserted in the TMS model, it can be further simplified into a quadratic equation. This equation is valid specifically for sodium chloride and is as follows:

$$0.9562\xi^2 + \frac{0.83712\xi}{(\sigma - 1)} + 4 - \left(\frac{2}{\sigma - 1}\right)^2 = 0 \quad (10)$$

## Analysis of the problem and the objectives of the work

Removal of heavy metals from wastewater is paramount in this our 21st century due to its recalcitrance, persistence, and tendency to build-up in living organism. In addition, heavy metals cannot be degraded or destroyed in the environment without proper separation. Heavy metals and its effects in the environment have previously been discussed in this research (Fu and Wang, 2011; Gherasim et al., 2015; Murthy and Chaudhari, 2008). Numerous approaches have been employed for the development of cheaper and more effective technologies, both to decrease the amount of wastewater produced and improve the quality of separation processes involved (Barakat, 2011). Diverse conventional technique has been carried out over the years to remove heavy metals from industrial effluents. But these methods have many setbacks as discussed earlier.

The aim of this research is to investigate the performance of two commercially available thin–film composite polyamide NF membranes (AFC 30 and AFC 80) for separating of toxic heavy metals from wastewater. Structural parameters and electrical parameter of the membranes were estimated. Experiments with neutral aqueous solutions in conjunction with two independent mathematical pore models (Donnan Steric Pore model – DSP model, and Steric Hindrance Pore model – SHP model) were performed at various process conditions. The fixed charge density on the membrane surface was determined from different concentrations of sodium chloride (NaCl) experiment by using the Spiegler–Kedem model together with the charge model called Teorell–Meyer–Sievers (TMS). In addition, the study disclosures the influence of different operating parameters to find the optimum condition for the removal of heavy metals from wastewater. These heavy metals to be considered are zinc sulphate ($ZnSO_4$), zinc nitrate ($Zn(NO_3)_2$), cobalt nitrate ($Co(NO_3)_2$) and nickel nitrate ($Ni(NO_3)_2$). The operating parameters evaluated are transmembrane pressure, feed concentration, cross–flow velocity and pH.

Modelling of heavy metal rejection was developed to select appropriate membrane, separation mechanism, design process, and improve the efficiency of membrane. Mathematical modelling plays a key role in the design and improves on efficiency of a membrane. This leads to a smaller number of experiments, saving time, and in–depth knowledge of the separation mechanism (Agboola et al., 2015). Several studies had

attained reliable results similar to Spiegler–Kedem model. Therefore, the Spiegler–Kedem model was used to evaluate the real rejection of heavy metals in all our experiments by finding the coefficient of reflection and solute permeability.
In summary, the objectives of my research are as follows;

- Evaluate the structural parameters (pore size and membrane porosity ratio) and electrical properties by modelling with DSPM model, SKM model with SHP model and SKM with TSM model.
- Evaluate the effect of operating variables for the removal of heavy metals (zinc, cobalt, and nickel) from wastewater.
- Modelling of rejection of heavy metals using Spiegler–Kedem model (SKM) and Steric Hindrance Pore (SHP) model.

# Experimental

## 4. Experimental System

Nanofiltration experiments were performed by a cross–flow separation unit whose scheme is depicted in Fig. 2. A tubular MIC-RO module which was manufactured by PCI membrane system was used to carry out the experiment. The module was equipped with two tubular NF membranes of 1.25 cm internal diameter and 30 cm length, the effective filtration area of 240 $cm^2$.

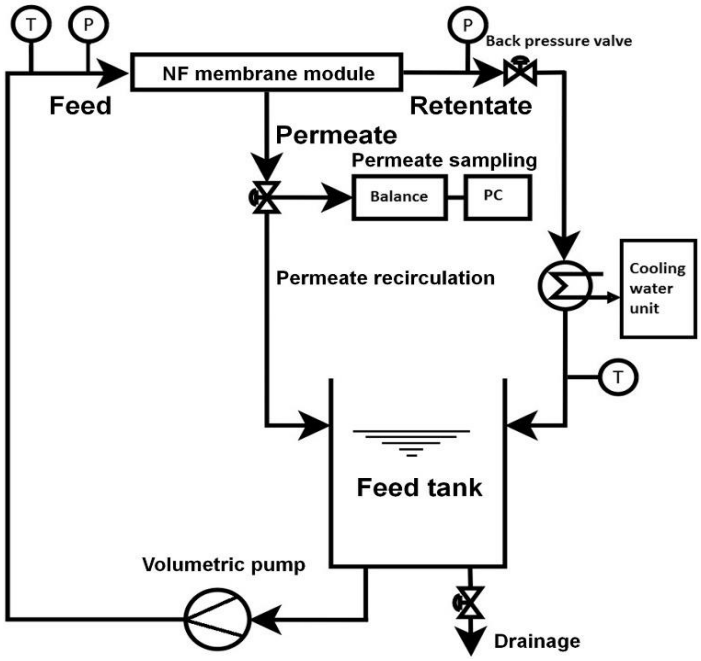


Fig. 2. Setup of nanofiltration experimental system

## 4.1 Membranes

Two kinds of NF tubular membrane (AFC 30 and AFC 80) from PCI membrane system were used in these experiments. These membranes are thin–film composite membrane consisting of aromatic polyamide skin-layer on polysulfone substrate. AFC 30 and AFC 80 membranes are capable of withstanding transmembrane pressures up to 60 bar, temperature below 70 $^oC$ and pH in 1.5–9.5 range.

### 4.2 Chemicals

All the reagents used were of analytical reagent grade or of highest purity. The aqueous solution was prepared by dissolving the following reagents: glucose, glycerol, triethylene glycol (TEG), lactose, ethanol, isopropyl alcohol, sec butyl alcohol, zinc sulphate ($ZnSO_4$), zinc nitrate ($Zn(NO_3)_2$), cobalt nitrate ($Co(NO_3)_2$), nickel nitrate ($Ni(NO_3)_2$), and sodium chloride (NaCl). It was supplied by Penta Co., the Czech Republic. The individual solutions were prepared by dissolving the respective reagents in highly demineralised water (conductivity < 1 μS/cm, pH 6.0 ± 0.2).

### 4.3 Analyses

Neutral solutes concentration in binary system was evaluated by TOC technique as total organic carbon. Heavy metals concentrations were analysed by ICP apparatus. Conductivity was measured by WTW Cond 340i conductometer for feed and WTW Cond 3210 conductometer for permeate equipped with a WTW 325 electrode, respectively. The pH was measured by HI 9126 pH-meter, Hanna Instruments).

## Results and discussions

### 5. Evaluation of structure parameters

The NF experiments for the membrane structural characterization of both membranes (AFC 30 and AFC 80) were performed with neutral solutes of 500 mg $L^{-1}$ solution. The pure water flux and the fluxes of the solutions used against transmembrane pressure difference is shown in Fig. 3.

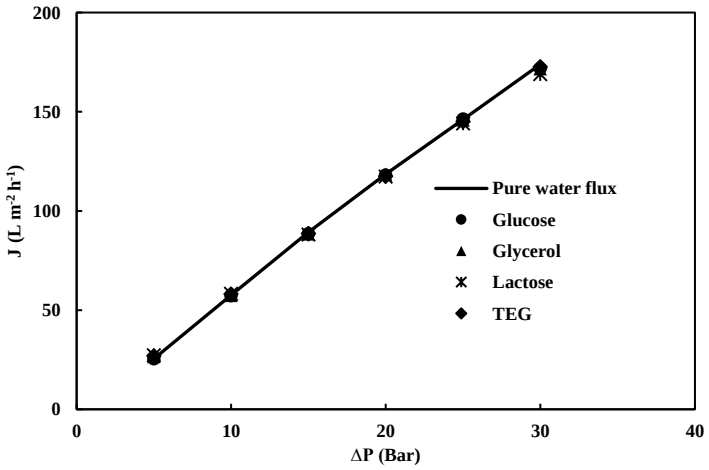


Fig. 3 Dependency of permeate flux on transmembrane pressure differences for neutral solutes. Pure water flux (solid lines), and neutral solutes (symbols). (a) AFC 30 and (b) AFC 80 membrane.

Both membranes pure water permeability was then calculated. The values of pure water permeability *($L_p$)* for both membranes (AFC 30 and AFC 80) at 25 ° C were 5.926 L $m^{-2}$ $h^{-1}$ $bar^{-1}$ and 1.526 L $m^{-2}$ $h^{-1}$ $bar^{-1}$, respectively. It has been observed that the flux linearly increases with increased transmembrane pressure difference for both membranes being considered. From differences in values of pure water permeability, it is clearly shown that AFC 80 membrane is denser than AFC 30 membrane.

## 5.1 Donnan Steric Partitioning model (DSPM)

By incorporating the expression for the thickness–to–porosity ratio into the Peclet number equation, a new expression is obtained for real rejection depending only on the pore radius. By fitting the experimental rejection value for different transmembrane pressures with the real rejection from model, the pore radius ($r_p$) can then be estimated for both membranes (AFC 30 and AFC 80) using the cylindrical pores. This is followed by the corresponding values for the membrane thickness to porosity ratio ($\Delta x/A_k$) which was calculated from Eq. (4) and presented in Table 1. The application of these equations assume that the transmembrane pressure drop is negligible through the microporous sublayer, implying that the transmembrane pressure drop can be attributed to the active layer, which is an assumption made in most literature (Lanteri et al., 2008).

Table 1. Estimation of structural parameters of NF membranes using DSP model

| **Membrane** | **Solutes** | **DSP model** | |
|---|---|---|---|
| | | $r_p$ (nm) | $\Delta x/A_k$ (μm) |
| **AFC 30** | Glycerol | 0.316 | 2.31 |
| | TEG | 0.365 | 3.08 |
| | Glucose | 0.355 | 3.18 |
| | Lactose | 0.503 | 5.89* |
| | **Average** | **0.343** | **2.86** |
| **AFC 80** | Ethanol | 0.212 | 4.17 |
| | Isopropyl alcohol | 0.245 | 5.53 |
| | Glycerol | 0.262 | 6.38 |
| | Sec butyl alcohol | 0.265 | 6.53 |
| | **Average** | **0.246** | **5.65** |

Also, NF membrane can be modelled using slit–like pores geometry. Selection of the neutral solutes for the experiment play a pivotal role to obtain values to fit the DSP model. One of the criteria with this method is choosing neutral solutes of varied sizes or nominal molecular weights closer to each other to assure similar interaction with the membrane. It is necessary since the differences in interaction with the membrane material can have a significant effect on the differences in the solute retention based on size exclusion (Garcia-Mintin et al., 2014). From our results, the neutral solutes chosen for both AFC 30 and AFC 80 are glucose and glycerol, respectively. This is because both pore sizes are closer to each membrane and fit very well with the experimental values. From Table 2, the pore size and thickness to porosity ratio for slit–like pore are 0.370 nm and 3.18 μm, respectively. The pore radius of glucose using slit like geometry was closer to the Stokes radius of glucose (0.355 nm) and fit very well with the experimental values (see Fig. 4).

Table 2. Structure parameters of AFC 30 and AFC80 membranes

| Membranes | Pore geometry | Membrane structural parameters | | Quality of fittings |
|---|---|---|---|---|
| | | $r_p$ (nm) | $\Delta x/A_k$ (μm) | ($\chi^2$) |
| **AFC 30** | Slit–like | 0.370 | 3.18 | $2.57\times10^{-4}$ |
| | Cylindrical | 0.486 | 2.05 | $8.42\times10^{-3}$ |
| **AFC 80** | Slit–like | 0.262 | 6.38 | $2.25\times10^{-6}$ |
| | Cylindrical | 0.329 | 3.23 | $2.38\times10^{-3}$ |

Wallace et al., (2017) used different neutral solutes to evaluate the structural parameters of AFC 30 membrane. Also, Gherasim et al., 2014 used four neutral solutes to determine the structural parameters of AFC 80 membrane. The authors found out that bundle of cylindrical pores fitted the experimental data and in good agreement when compared to the assumption of slit–like pores. This condition is valid when the average pore sizes of different neutral solutes is used. Other studies confirm that, NF membrane can be modelled using the cylindrical pore geometry (Gherasim and Mikulášek, 2013; Bouranene et al., 2009). Therefore, NF membrane can be modelled by DSP model using either slit–like or cylindrical pores. In case of slit–like pore, the pore radius value found should be closer to the stoke radius of the neutral solute. When such results are achieved, the experimental values will fit very well to the DSP model. In terms of using different neutral solutes, the average of the pore radius should be used by evaluating with the cylindrical pores. Selection of the neutral solutes for the experiment play a pivotal role to obtain values to fit the DSP model. One of the criteria with this method is choosing neutral solutes of varied sizes or nominal molecular weights closer to each other to assure similar interaction with the membrane. It is necessary since the differences in interaction with the membrane material can have a significant effect on the differences in the solute retention based on size exclusion (Garcia-Martin et al., 2014).

Also, the rejections of the neutral solutes of both membranes (AFC 30 and AFC 80) were compared to the two independent models (DSPM and SHP). It was observed from Fig. 4 that, the two independent models fit well with the experimental results of all the neutral solutes. The observed solute rejections increase continuously with increasing of permeate flux for neutral solutes which can be seen in Fig. 4. Selection of neutral solutes for the determination the pore radius is important when considering the molecular weight of each solute. Solutes with close molecular weight will help achieve better results of pore radius and membrane porosity ratio. The SHP is not a good model for solutes with reflection coefficient very close to unity or highly restricted permeation. For instance, lactose has high rejection close to unity and this model is not useful for this solute (Nakao and Kimura, 1982).

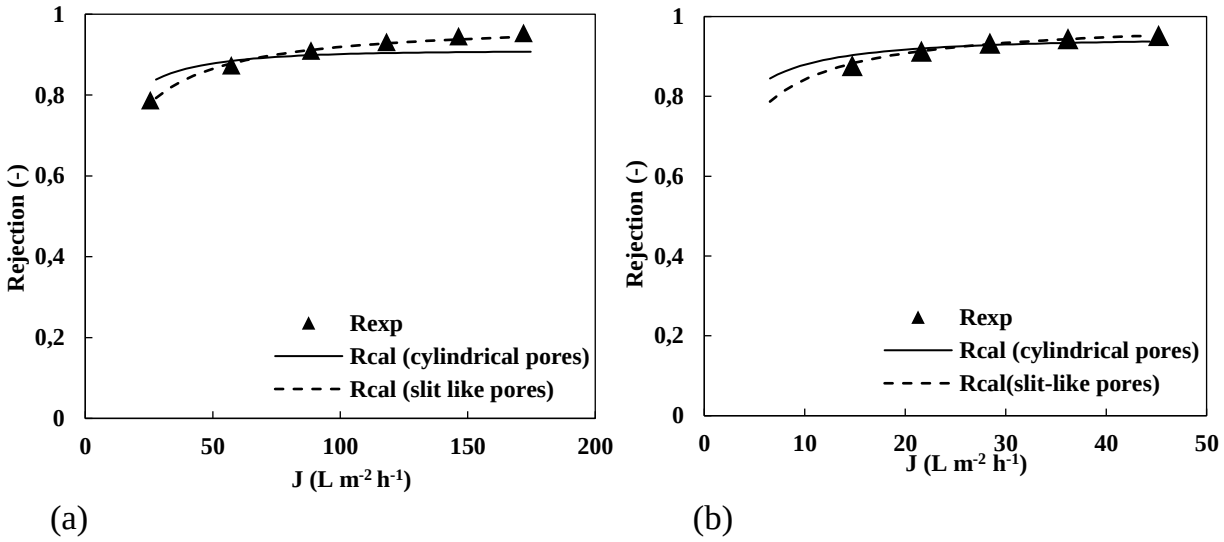


Fig. 4. Experimental data by (a) AFC 30 membrane for glucose and (b) AFC 80 membrane for glycerol. Experimental rejection (symbol), cylindrical pores geometry (full line), and slit–like pores (dotted line).

From our results, the molecular weight cut–off (MWCO) which corresponds to 90 % rejection of solutes is for AFC 30 between molecular weight of triethylene glycol and glucose and AFC 80 between ethanol and isopropyl alcohol. We can assume that the molecular weight cut–off (MWCO) of AFC 30 is approximately 150 g mol$^{-1}$ and 60 g mol$^{-1}$ for AFC 80 membrane. By using interpolation, the obtained values are 153 g mol$^{-1}$ (AFC 30) and 59.8 g mol$^{-1}$ (AFC 80), respectively.

### 5.2 Steric Hindrance Pore model (SHP)

The structural properties ($r_p$ and $\Delta x/A_k$) were determined by using the following steps. First, the real rejection against the volume flux was used to estimate the membrane parameters (σ and $P$) by the *chi–test* method to get best fit using the Spiegler–Kedem model found in Eqs. (6) and (7). Both (AFC 30 and AFC 80) membranes values of the parameters can be found in Table 3. Then using Eq. (10) which was based on SHP model from reflection coefficients of different neutral solutes (Nakao and Kimura, 1982) and error function method, λ of each neutral solute is determined. Since λ is the ratio of the solute radius ($r_s$) to pore radius ($r_p$), and the solute radius are known, the pore radius of each neutral solutes can be calculated. Also, the membrane porosity ratios ($\Delta x/A_k$) were evaluated using Eq. (7) as the solute permeability of each neutral solutes and λ are known for both NF membranes.

Table 3. Estimation of structural parameters of NF membranes using SHP model

| Membrane | Solutes | SHP model | | | |
|---|---|---|---|---|---|
| | | σ (-) | P $10^{-6}$ m $s^{-1}$ | $r_p$ nm | Δx/Ak μm |
| **AFC 30** | Glycerol | 0.774 | 19.50 | 0.342 | 2.94 |
| | TEG | 0.915 | 4.20 | 0.389 | 3.21 |
| | Glucose | 0.950 | 1.64 | 0.392 | 3.65 |
| | Lactose | 0.992 | 0.20 | 0.522 | 4.32* |
| | **Average** | | | **0.374** | **3.27** |
| **AFC 80** | Ethanol | 0.914 | 4.32 | 0.229 | 5.36 |
| | Isopropyl Alcohol | 0.983 | 0.68 | 0.256 | 5.39 |
| | Glycerol | 0.981 | 0.52 | 0.275 | 6.74 |
| | Sec butyl alcohol | 0.984 | 0.45 | 0.276 | 6.54 |
| | **Average** | | | **0.259** | **6.00** |

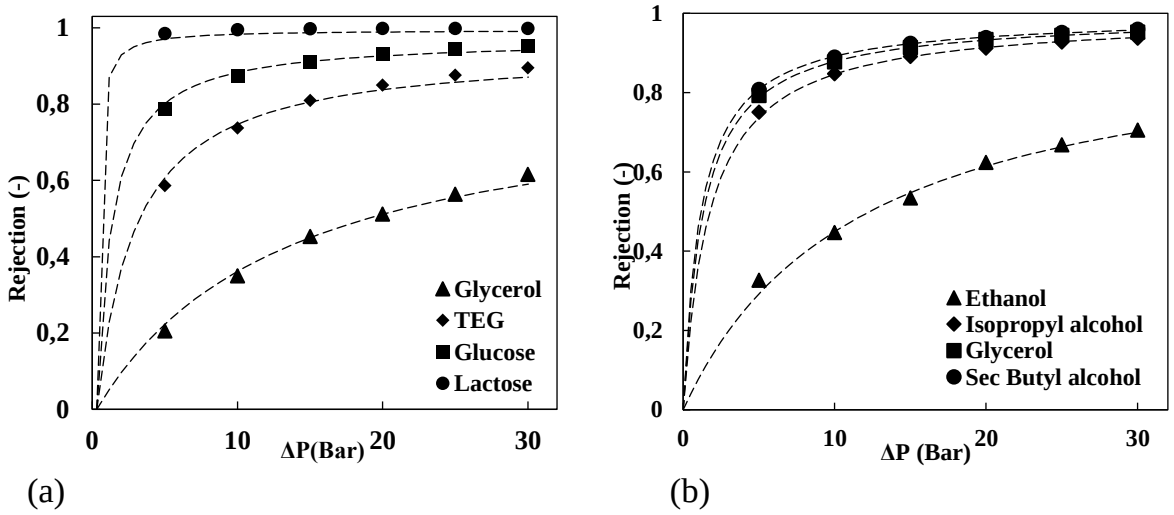


Fig. 5. Rejection of neutral solutes as a function of transmembrane pressure differences for membranes (a) AFC 30 and (b) AFC 80 using two independent models. DSPM (symbols) and SHP (dashed lines).

## 5.3 Membrane charge density

The membrane charge is an important parameter useful in the NF process. This is because the separation mechanism is a combination of size exclusion and electrical interaction (repulsion forces) between the ions in the feed (retentate) and the charged membrane. In addition, the membrane charge allows one to estimate, explain, and model the respective NF processes.

The membrane charge is determined by the type or chemical structure of the membrane material and is due to dissociation of the functional group(s) present in the membrane material, or adsorption of different charge or polarizable solutes from the solution (Gherasim et al., 2014). The AFC 30 membrane has a polyamide outer layer which gives rise the formation of ammonium ($–NH_3^+$) and carboxyl (–COOH) group. The isoelectric point is at pH about 5.3 (AFC 30 membrane) and 3.6 (AFC 80 membrane) in KCl solution (Bouranene et al., 2008; Mikulášek and Cuhorka, 2016). If the pH<IEP the membrane is positively charged as the carboxyl groups are

undissociated and the amino groups are protonated. Likewise, membrane is negatively charge at pH>IEP as the carboxyl groups are dissociated.

To estimate the membrane charge, different experiments were performed for NaCl solutions with various concentrations from 100–4500 mg $L^{-1}$. It has been observed that the permeate flux slightly decreases with increasing in NaCl concentration, which can be explained because of the increased osmotic pressure.

Table 4 depict that the Spiegler–Kedem model describes a very well the experimental rejection data for all NaCl concentrations considered. As can be observed in Fig. 5, the reflection coefficient (σ) decreases and the solute permeability (*P*) increases by increasing the salt concentration in the feed solution. This is in good agreement with the gradually decreasing rejection when increasing NaCl concentrations of the solutions obtained experimentally as shown in Fig. 6. The Spiegler–Kedem model can estimate a good description of the experimental results of NaCl rejection.

Table 4. Reflection coefficients (σ) and solute permeabilities (*P*) determined by fitting experimental data of NaCl rejection with Spiegler–Kedem model (AFC 30)

| **NaCl concentration** | **Spiegler–Kedem model parameters** | | **Effective fixed charge density** | **Quality of fitting** |
|---|---|---|---|---|
| mg $L^{-1}$ | σ (-) | P (L $m^{-2}$ $h^{-1}$) | -ΦX (mV) | $\chi^2$ |
| 100 | 0.940 | 9.071 | 48.8 | $1.230\times10^{-4}$ |
| 200 | 0.936 | 10.967 | 87.9 | $9.247\times10^{-5}$ |
| 500 | 0.903 | 16.585 | 144.0 | $1.081\times10^{-4}$ |
| 1000 | 0.873 | 28.366 | 211.2 | $1.303\times10^{-4}$ |
| 4500 | 0.781 | 67.300 | 564.0 | $4.145\times10^{-4}$ |

The dependence of the effective fixed charge density (Φ*X*) of AFC 30 membrane can be seen in Fig. 6 on various NaCl concentrations in the feed solution. It was observed that the membrane charge is strongly dependent on the concentration in the feed solution which was in contact to the membrane. The membrane charge was increasing when NaCl concentration of the solution increases. From the experimental results, the increase in the negative membrane charge can be explained by the adsorption of chloride ions on the membrane. A detailed explanation of AFC 80 membrane to estimate fixed charge density using TMS together with NaCl concentration has been performed by Gherasim et al., 2014. The authors observed that the membrane charge is strongly dependent on the concentration of the solution with which the membrane is in contact; the membrane negative charge is increasing monotonically when the NaCl concentration in the aqueous solution increases. This behaviour was attributed to the adsorption of ions from solution on the membrane surface. Other authors observed had similar trend which can be attributed to adsorption of ions from the solution to the membrane surface (Schaep et al., 1999; Bowen and Mukhtar, 1996; Zydney, 1997; Wang et al., 2012).

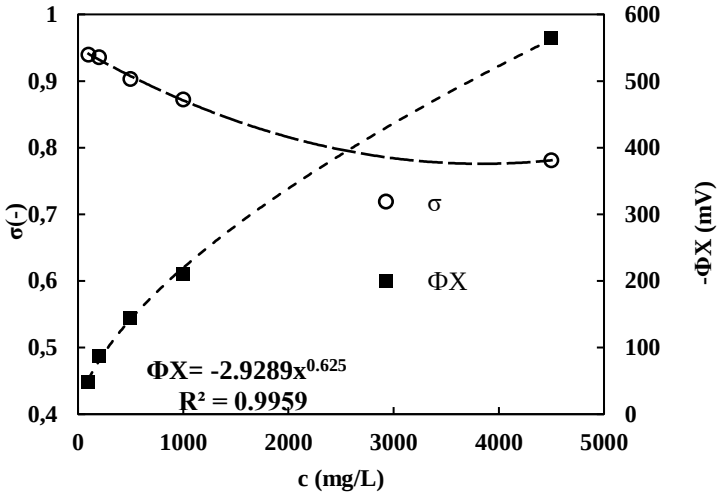


Fig. 6. Reflection coefficient and effective fixed charge density of AFC 30 membrane as a function of NaCl concentration in the feed solution. Effective charge density was fitted with Freundlich isotherm (dashed line).

## 6. Influence of operating parameters on heavy metals separation

To select the optimum operating parameters for NF membrane, it is advisable to change operating conditions such as applied transmembrane pressure, feed concentration, cross–flow velocity, and pH. This is a useful technique used to investigate the transfer of solute as well as the separation properties of the membranes. Therefore, performing experimental works on these operating parameters is important to predict the extent of heavy metals that can be concentrated in retentate.

### 6.1 Influence of transmembrane pressure and feed concentration

For a better understanding of NF membrane process, the influence of different applied transmembrane pressure on the rejection of heavy metals was investigated for each membrane (AFC 30 and AFC 80). This was done by carrying out retention experiments with transmembrane pressure difference (5–30 bar) at constant cross–flow velocity of 1.25 m $s^{-1}$.

Some remarks can be made based on the results of the transport mechanism of solutes in NF membrane process. As presented in Fig. 7 and Fig. 8, increase in transmembrane pressure differences gradually increases the rejection for all heavy metals for both membranes being considered. The maximum rejection of all heavy metals was at a transmembrane pressure of 30 bar for AFC 30 and AFC 80 membranes. Therefore, the rejection increases with increasing transmembrane pressure due to dilution effect, as the higher solvent flux would result in the dilution of permeate and hence in higher rejection (Seidel et al., 2002). In the case of AFC 30 membrane, the minimum rejections were almost 30 % (cobalt nitrate), followed by 44 % (nickel nitrate) for a transmembrane pressure of 5 bar. Also, it was observed that the minimum rejection of nickel nitrate is higher than zinc nitrate at feed concentration of 200 mg $L^{-1}$ at 5 bar. The maximum rejection was above 99 % (zinc sulphate) and even minimum rejection of 95 % at 5 bar. Although zinc nitrate has the higher rejection than nickel nitrate, it has minimum rejection than nickel nitrate at 5 bar with 200 mg $L^{-1}$ feed concentration. For AFC 80 membrane, the maximum rejection was obtained at 30 bar for all heavy

metals considered (see Fig. 8). The rejections of zinc sulphate, cobalt nitrate, zinc nitrate, and nickel nitrate were 99.1, 98.9, 98.6, and 98.1 %, respectively at a feed concentration of 200 mg $L^{-1}$. The lowest rejection was almost 97 % for a transmembrane pressure of 10 bar for all heavy metals at 50 mg $L^{-1}$ (see Fig. 8).
Among the heavy metals considered, the maximum rejection was zinc sulphate for both membranes. It could be explained that the different in the rejection when compared to the rest of the heavy metal in our case was due to divalent ions (sulphate) present in the zinc. This is because of less repulsion forces of the membranes pushing them away from the membrane surface. Usually, concentration polarization and the shielding of the charged membrane at high feed concentrations determine a decrease in rejection. Nevertheless, it was observed that rejection rate increases with feed concentrations of all heavy metals considered for both membranes. The results found in our case is not common. Increasing the feed concentration increases the rejection due to adsorption of ions on the membrane surface. This means that the membrane becomes positively charged and in turn leads to more retention of ions (Mehdipour et al., 2015).

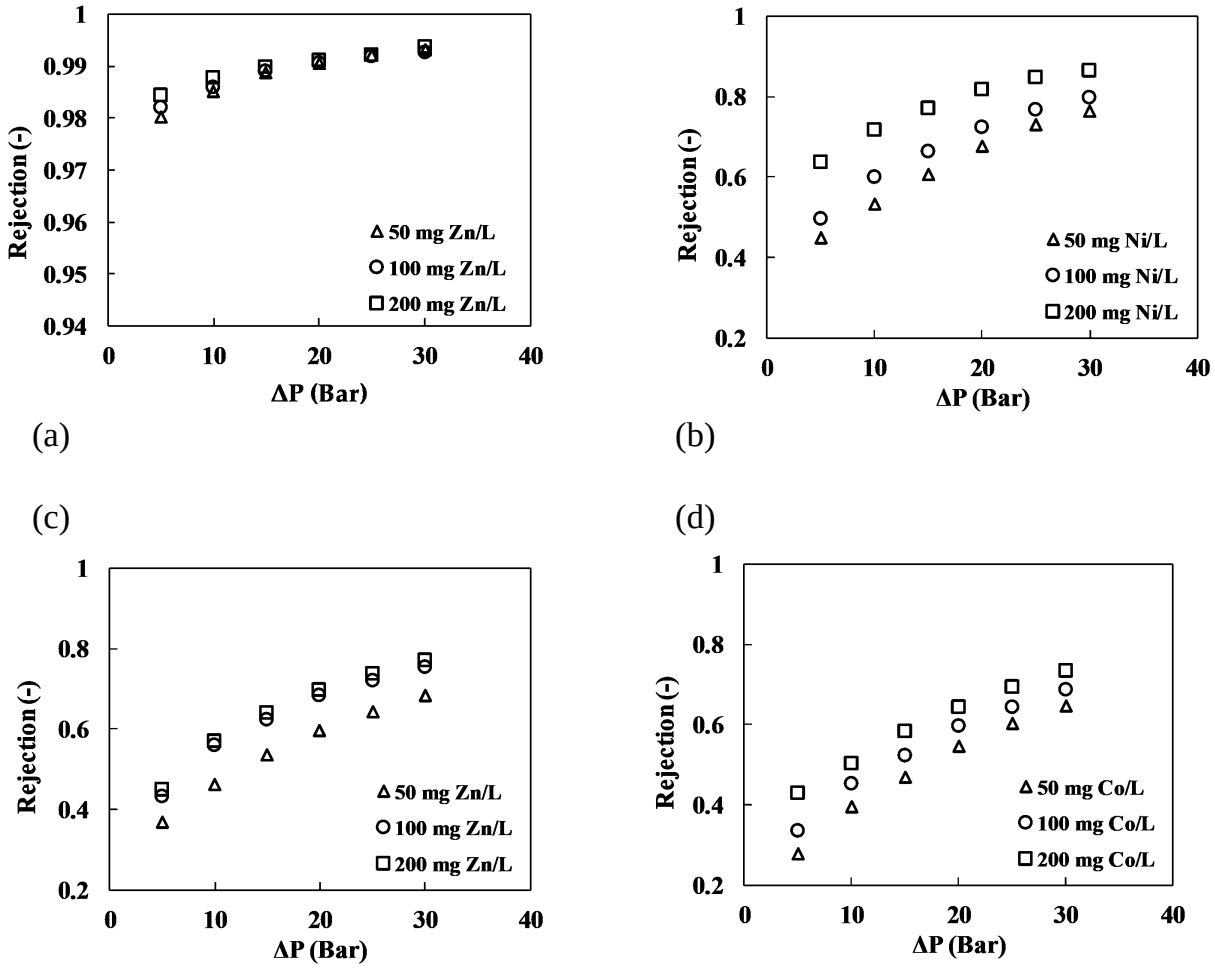


Fig. 7. Rejection as a function of transmembrane pressure for AFC 30 membrane with various feed concentrations (a) zinc sulphate (b) nickel nitrate (c) zinc nitrate (d) cobalt nitrate.

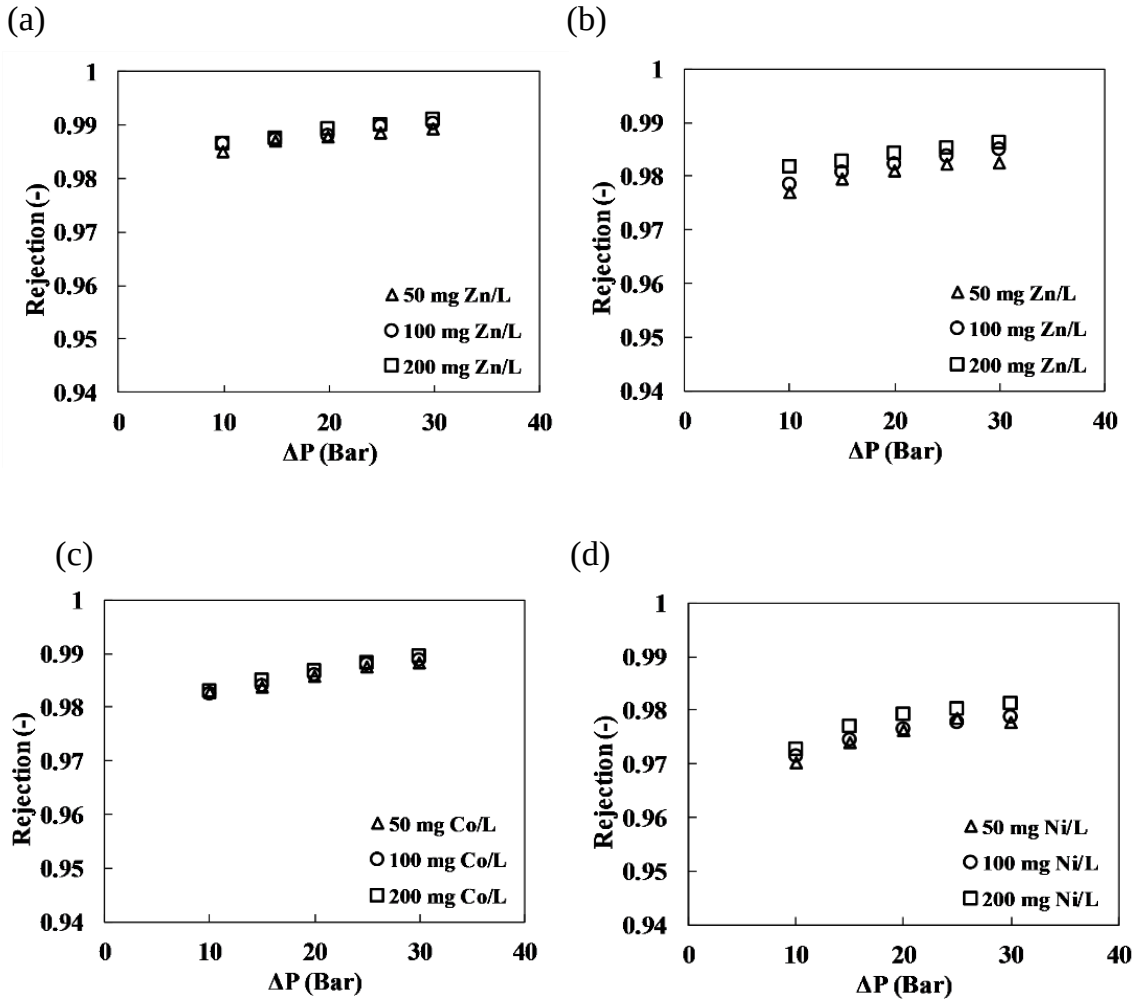


Fig. 8. Rejection as a function of transmembrane pressure for AFC 80 membrane with various feed concentrations (a) zinc sulphate (b) zinc nitrate (c) cobalt nitrate (d) nickel nitrate.

## 6.2 Influence of pH

One of the important parameters of the NF membrane is the pH of the solution. However, enough information is not provided by the manufacturer about the membrane charge which can be useful in characterization of a membrane. The pH of the feed influences the membrane charge and then the rejection properties of NF membrane. The type of chemical structure of the membrane material determines the membrane charge. Change of charge is due to dissociations of the functional group of the membrane material, or adsorption of charge polarizable solutes (cations or anions) from the solution (Bouranene et al., 2009; Gherasim et al., 2013). Both AFC 30 and AFC 80 membrane used has a polyamide top layer and amphoteric character. The partial hydrolysis of polyamide leads to formation of ammonium ($–NH_3^+$) and carboxyl (–COOH) groups. When the membrane is below the IEP, the carboxyl groups are dissociated, and the amino group are protonated, the membrane charge is positive. On the other hand, when the membrane is above the IEP the carboxyl group are dissociated and the membrane is charged negatively. Szymcyzk et al., 2007 performed experiment with KCl solution and found out that IEP of AFC 30 membrane was at pH about 5.3. The same behaviour was found for AFC 80 membrane. Because Gherasim

et al., 2013 performed experiment with solution of $Pb(NO_3)_2$ and found out that the IEP of AFC 80 membrane was shifted from pH of 3.6 to a higher value of about 5.7.
The influence of pH on rejection was considered for feed solution of 50 mg Zn/L with pH (5.3, 6.0, 6.5) adjusted by $H_2SO_4$. From our result in Fig. 9, it can be observed that rejection of zinc ion of AFC 30 membrane was very high for all pH range considered. Rejection slightly increases with increasing in pH value. At isoelectric point with pH 5.3, the membrane is uncharged which makes a solute rejection of 96.8 % at 30 bars. In addition, AFC 30 membrane has pores (0.374 nm) which are much larger than Stokes radii of zinc and sulphate ions. These Stokes radii are 0.348 nm and 0.229 nm respectively. Comparing the pores radius of AFC membrane to that of Stokes radii of the ions, we can deduce that the zinc ions will be retained more than sulphate ions. This shows that AFC 30 membrane is governed by steric hindrance in our case otherwise, the reverse order would be expected. It can be expected that the steric effect plays a major role in rejection with respect to the electric interaction (Mehdipour et al., 2015). When the pH values (6.0 and 6.5) are above IEP, the carboxyl groups are dissociated, and the membrane becomes more negatively charged which increases the rejection of zinc ions. The maximum rejection of 98.7 % was reached at the highest value of pH at 30 bar. This behaviour could be explained by a decrease in pore size dimension when the membrane is charged by the increased repulsion between the charged functional groups of the membrane (Childress and Elimelech, 2000). In our case, the electrostatic repulsion that occurs between the zinc ions and charged membrane in turn increase the rejection rate with increase in pH (see Fig. 9). This finding could be used in explaining the different heavy metals considered in our case.

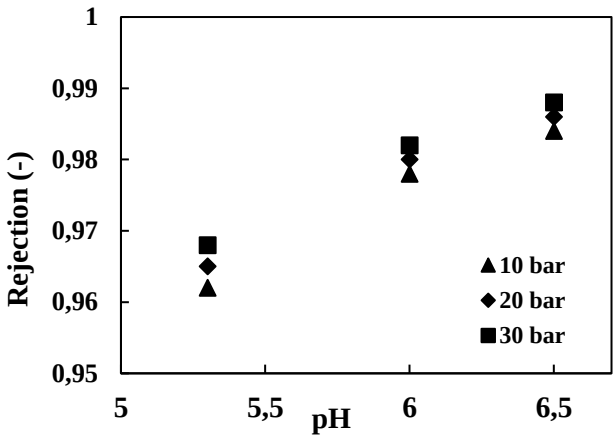


Fig. 9. Observed rejection against pH for $ZnSO_4$ feed solution with concentration of 50 mg Zn $L^{-1}$ at different applied transmembrane pressure.

### 6.3 Influence of cross–flow velocity

One of the major drawbacks in NF membrane separation is the concentration polarization phenomenon. This phenomenon reduces the membrane performance process by increasing the osmotic pressure at the membrane surface due to the accumulation of retained solutes near the membrane on the high–pressure side. During the process, the concentration of solutes at the membrane surface is higher than in the bulk of the feed, and a boundary layer is builds up as a result of the equilibrium

established between the transport of solutes towards the membrane by convection and the slower back diffusion of the retained species. The concentration polarization phenomenon affects the flux, the retention and the fouling of the membranes which limit in the application of NF treatment of highly feed concentration side (Gherasim et al., 2015; Bowen et al., 1997; Bowen and Mukhtar, 1996; Sablani et al., 2001).

The influence of the cross–flow velocity was investigated and applied with the aim to create a high shear condition at the surface of the membrane (Bian et al., 2000). The feed flow rate through the tubular NF membrane was set at 0.420, 0.833, and 1.250 m $s^{-1}$ with concentration of feed solution chosen for these experiments as 100 mg Zn $L^{-1}$ (zinc sulphate and zinc nitrate). For calculation of real rejections, the solution properties (density and viscosity) were considered as identical to those of pure water which is valid for dilution solutions.

The difference between the observed and real rejections decreases when increasing the cross–flow velocity as seen in Fig. 10. The equivalent calculated Reynolds numbers from the cross–flow velocities of 0.420, 0.833 and 1.250 m $s^{-1}$ are 5890, 11,670, and 17,500, respectively. The calculated Reynolds numbers are greater than 2000 at all cross–flow velocity which guarantee a turbulent flow in the membrane module (AFC 30) under investigation. By using Eq. 8, diffusion coefficient ($D$) of zinc nitrate and zinc sulphate was calculated as $2.51 \times 10^{-6}$ and $8.47 \times 10^{-6}$ $m^2$ $s^{-1}$, respectively. The mass transfer coefficients of zinc nitrate and zinc sulphate in the polarization layer ($k$) were found using Eq. 7. Table 5 shows the values of mass transfer coefficient of both zinc sulphate and zinc nitrate at different cross–flow velocity. It can be observed that the mass transfer coefficient increases as the cross–flow velocity increase.

Table 5. Mass transfer coefficients at various cross–flow velocities

| **Cross–flow velocity** | **Mass transfer coefficient** | |
|---|---|---|
| | **Zinc nitrate** | **Zinc sulphate** |
| m $s^{-1}$ | $k \times 10^{-5}$ $m^2$ $s^{-1}$ | |
| 0.420 | 1.05 | 2.47 |
| 0.833 | 1.94 | 4.57 |
| 1.250 | 2.78 | 6.52 |

As described in Fig. 10 (b), real rejection increases with increase in permeate flux at constant cross–flow velocity. Furthermore, as the cross-flow velocity of the feed solution increases the difference between observed and real rejection decreases. At the lowest cross–flow velocity of 0.42 m $s^{-1}$, the observed rejection decreases when increasing the applied transmembrane pressure (see Fig. 25). This could be explained that more solutes (in our case zinc sulphate and zinc nitrate) are transported to the membrane by convection as the transmembrane pressure increases and eventually accumulates near the membrane. Due to the low cross–flow velocity, the concentration polarization increases and decreases the observed rejection significantly. Differences in observed and real retention give clear indication that the concentration polarization effect decreases when increasing the cross–flow velocity. From Table 5, it was observed that the mass transfer coefficient in the polarization increases when increasing the feed flow rate from 0.42 to 1.25 m $s^{-1}$. The reason for the increase in the mass transfer coefficient in the polarization layer is because of the decrease in the thickness of the boundary layer in the membrane surface when increasing the cross–flow velocity. From our results obtained, we possibly conclude that enhancing the

hydrodynamics by increasing the cross–flow velocity decreases the concentration polarization of AFC 30 membrane. This will lead to increasing of rejection and permeate flux. The maximum real rejection of both zinc nitrate and zinc sulphate (see Fig. 10) are above 95 % which proves that the membrane has a good property for the separation of heavy metals. The minimum real rejection of zinc nitrate was about 52 % compared to 97 % of zinc sulphate.

Regarding AFC 80 membrane, Gherasim and Mikulášek, 2014, studied the influence of cross–flow velocity on the removal of heavy metal by nanofiltration. The authors found that the metal rejection (250 mg Pb $L^{-1}$ at pH 5.8) slightly increases with increase in feed cross–flow velocity. The increase of rejection was explained by differences in concentration polarization and mass transfer coefficient.

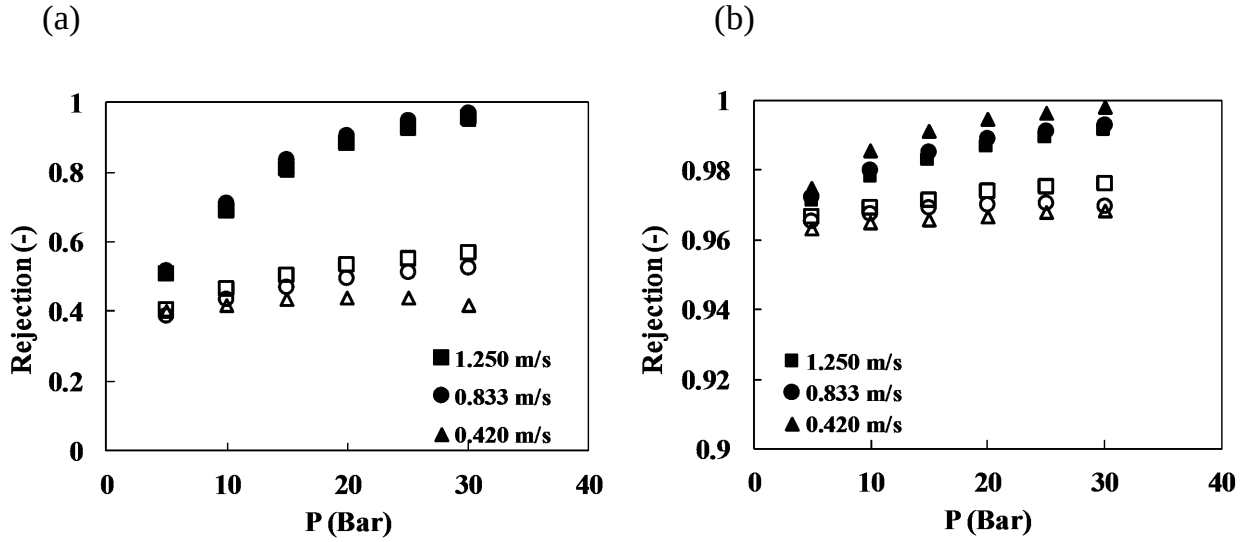


Fig. 10. Rejection of AFC 30 membrane as a function of cross–flow velocity (a) zinc nitrate (b) zinc sulphate (observed rejections – empty symbols, real rejection – full symbols).

## 7. Modelling of heavy metals rejection

### 7.1 Spiegler–Kedem model (SKM)

The experimental rejections were fitted with the Spiegler–Kedem model to give more information about the membranes used (AFC 30 and AFC 80). The experimental data together with the model prediction are plotted as seen in Table 6 and Table 7. The heavy metal considered was zinc sulphate, zinc nitrate, cobalt nitrate, and nickel nitrate for both membranes.

In terms of AFC 30 membrane, it was observed that model shows with high accuracy the experimental rejection of heavy metals for all feed concentration. The high rate of reflection coefficients (σ) and low solute permeability ($P$) were estimated by fitting the experimental data with the Spiegler–Kedem model which agrees with the rate of rejection as presented in Table 6. As can be seen in Table 6, the feed concentration increases when the reflection coefficients gradually decrease and the membrane permeabilities slightly increases for only zinc sulphate. In our case, an opposite trend was found for the rest of the heavy metals being considered (see Table 6). The

reflection coefficients increase whiles the solute permeability decreases for zinc nitrate, cobalt nitrate, and nickel nitrate with increasing concentration.

Table 6. Reflection coefficients (σ) and solutes permeabilities (P) obtained by fitting of experimental data using the Spiegler–Kedem model for AFC 30 membrane

| Solute | Concentration (mg $L^{-1}$) | Reflection coefficient σ (-) | Solute permeability P (L $m^{-2}$ $h^{-1}$) | Quality of fittings ($\chi^2$) |
|---|---|---|---|---|
| Zinc sulphate | 50 | 0.997 | 0.82 | $1.58 \times 10^{-6}$ |
| | 100 | 0.995 | 1.20 | $2.05 \times 10^{-7}$ |
| | 200 | 0.993 | 1.36 | $1.42 \times 10^{-7}$ |
| Zinc nitrate | 50 | 0.875 | 21.70 | $3.92 \times 10^{-2}$ |
| | 100 | 0.926 | 15.20 | $4.81 \times 10^{-3}$ |
| | 200 | 0.952 | 8.10 | $1.59 \times 10^{-2}$ |
| Nickel nitrate | 50 | 0.773 | 24.34 | $1.24 \times 10^{-2}$ |
| | 100 | 0.807 | 20.23 | $1.06 \times 10^{-3}$ |
| | 200 | 0.857 | 11.29 | $7.43 \times 10^{-4}$ |
| Cobalt nitrate | 50 | 0.753 | 51.92 | $6.51 \times 10^{-3}$ |
| | 100 | 0.796 | 44.02 | $1.38 \times 10^{-3}$ |
| | 200 | 0.827 | 23.97 | $8.49 \times 10^{-3}$ |

As can be seen in Table 6, the feed concentration increases when the reflection coefficients gradually decrease and the membrane permeabilities slightly increases for only zinc sulphate. In our case, an opposite trend was found for the rest of the heavy metals being considered (see Table 6). The reflection coefficients increase whiles the solute permeability decreases for zinc nitrate, cobalt nitrate, and nickel nitrate with increasing concentration.

Table 7. Reflection coefficients (σ) and solutes permeabilities (P) obtained by fitting of experimental data using the Spiegler–Kedem model for AFC 80 membrane

| Solute | Concentration (mg $L^{-1}$) | Reflection coefficient σ (-) | Solute permeability $P$ (L $m^{-2}$ $h^{-1}$) | Quality of fittings ($\chi^2$) |
|---|---|---|---|---|
| Zinc sulphate | 50 | 0.995 | 0.129 | $2.32 \times 10^{-6}$ |
| | 100 | 0.992 | 0.157 | $1.83 \times 10^{-6}$ |
| | 200 | 0.991 | 0.175 | $2.47 \times 10^{-6}$ |
| Zinc nitrate | 50 | 0.995 | 0.355 | $8.05 \times 10^{-5}$ |
| | 100 | 0.992 | 0.368 | $1.33 \times 10^{-5}$ |
| | 200 | 0.985 | 0.385 | $2.59 \times 10^{-5}$ |
| Nickel nitrate | 50 | 0.983 | 0.258 | $7.79 \times 10^{-6}$ |
| | 100 | 0.980 | 0.302 | $4.20 \times 10^{-6}$ |
| | 200 | 0.979 | 0.343 | $7.19 \times 10^{-5}$ |
| Cobalt nitrate | 50 | 0.994 | 0.234 | $5.40 \times 10^{-5}$ |
| | 100 | 0.992 | 0.252 | $4.56 \times 10^{-6}$ |
| | 200 | 0.989 | 0.279 | $1.17 \times 10^{-5}$ |

For AFC 80 membrane, the reflection coefficients (σ) decreases as the solute permeability ($P$) increase for all heavy metals considered (see Table 7). Mikulášek and Cuhorka, 2016, studied the removal of lead nitrate with different feed concentration (25, 150, 400 mg Pb $L^{-1}$) from aqueous solution. The authors fit the experimental data with the Spiegler–Kedem model. It was observed that the reflection coefficients slightly decrease as the feed concentration increases, thus predicting a decrease in the

rejection with increase in feed concentration. Similar results were obtained by several authors (Gherasim et al., 2015; Gherasim and Mikulášek, 2013). Therefore, the Spiegler–Kedem model can explain and predict NF process of heavy metals by both membranes over a wide range of concentration.

### 7.2 Steric Hindrance Pore model (SHP)

The effective pore radius for each heavy metal at 200 mg $L^{-1}$ was calculated from the transport parameters based on SHP model and was presented in Table 8. The pore radii of these membranes were calculated using the Stokes radius of the heavy metals. These Stokes radii were 0.290, 0.202, 0.210, 0.198 nm for $ZnSO_4$, $Zn(NO_3)_2$, $Ni(NO_3)_2$, and $Co(NO_3)_2$, respectively. By obtaining the membrane transport parameters, the SHP model was used to determine the effective pore radii of these membranes calculated using stokes radius of each heavy metals tested. It was found that the effective pore radius was similar to each other considering both membranes (AFC 30 and AFC 80) in our case. Since the reflection coefficient is almost close to unity for AFC 80 membrane (see Table 8), the pore radius will be similar. This is because the equation of the SHP determines the effective pore radius with the reflection coefficient. The effective pore is not physical true since the membrane absorbed the ions which in turn may change the charge and eventually decrease the pores. Both membranes show better rejection for divalent ions since the reflection coefficient was higher compared to monovalent ions. A similar result was achieved when different polyamide membranes were studied (Nair et al., 2018).

Table 8. Calculated of σ, λ, and $r_p$ values for heavy metals for both membranes

| **Membranes** | **Heavy metals** | **σ (-)** | **λ (-)** | **$r_p$ (nm)** |
|---|---|---|---|---|
| **AFC 30** | $ZnSO_4$ | 0.966 | 0.966 | 0.300 |
| | $Zn(NO_3)_2$ | 0.924 | 0.959 | 0.210 |
| | $Ni(NO_3)_2$ | 0.868 | 0.969 | 0.217 |
| | $Co(NO_3)_2$ | 0.855 | 0.964 | 0.214 |
| **AFC 80** | $ZnSO_4$ | 0.990 | 0.985 | 0.294 |
| | $Zn(NO_3)_2$ | 0.985 | 0.948 | 0.213 |
| | $Ni(NO_3)$ | 0.979 | 0.940 | 0.223 |
| | $Co(NO_3)_2$ | 0.989 | 0.955 | 0.220 |

## Conclusions

In this study, both NF membranes (AFC 30 and AFC 80) have been characterized by modelling of rejection experiment of different neutral solutes. The structural parameters — pore radius ($r_p$) and membrane thickness–to–porosity ratio ($\Delta x/A_k$) — were calculated by using two independent models (SHP and DSP). Based on the obtained results, the structural parameters prove to be useful as the data fit well with the experimental values of different neutral solutes for both AFC 30 and AFC 80 membranes. It was observed that the pore radius of neutral solutes using DSP model can be calculated as slit–like or cylindrical geometry. One important criterium is the selection of the neutral solutes used for modelling. Selection of neutral solutes for the determination the pore radius is important when considering the molecular weight of each solute. Solutes with close molecular weight will help achieve better results of

pore radius and membrane porosity ratio. However, the SHP model cannot be applied to neutral solute with reflection coefficient almost close to unity. The pore radii ($r_p$) for AFC 30 membrane and AFC 80 membrane were (0.340–0.375 nm) and (0.245–0.265 nm), respectively. In addition, the membrane porosity ratio ($\Delta x/A_k$) were in the ranges (2.80–3.50 μm) and (5.60–6.50 μm) for AFC 30 membrane and AFC 80 membrane. From our results, the two independent models can be used to predict and interpret the structural properties of NF membrane using different neutral solutes. The fixed charge density on the membrane surface was determined using sodium chloride experiments with different concentrations. The data from sodium chloride experiment were used to calculate the effective charge density ($\Phi X$) by using Spiegler–Kedem model together with the charge model called Teorell–Meyer–Sievers (TMS). It was revealed that the membrane charge depends solely on the salt concentration in the solution which is because of ion adsorption on the membrane surface. It was found that the charge density gradually increases with increasing of solution concentration which was described by the Freundlich isotherm.

The influence of transmembrane pressure, feed concentration, pH, and cross–flow velocity on heavy metal separation were examined. As observed, a linear relationship was found between transmembrane pressure and fluxes. Also increase in feed concentration slightly increase heavy metals rejection for both membranes. Similar trend was observed when increasing the transmembrane pressure. It was seen that real rejection increases with increase in permeate flux at constant cross–flow velocity. Also, as the cross–flow velocity of the feed solution increases, the difference between observed and real rejection decreases. The pH was found to influence both the rejection and the permeation flux since the charge properties of the surface layer of the NF membrane change with pH. From our results, it was observed that the divalent anions ($SO_4^{2-}$) was strongly rejected by the negatively charged functional groups of membrane compared to monovalent anions ($NO_3^-$) for different cations ($Co^{2+}$, $Zn^{2+}$, $Ni^{2+}$) for both membranes. For our case, both membranes exhibited a maximum rejection above 99 % for zinc sulphate. This was due to the growing repulsion between the membrane surface and higher valence ions. We can deduce that rejection is a very complex mechanism where the cations types, cations concentration, membrane charge could play their perspective role among other factors during nanofiltration separation process effects. Also, it was found that the difference of cations with equal valences is always associated to hydration energies of cations, their hydrated radii, and diffusivities of ions. Membrane transport parameters were found by fitting the Spiegler–Kedem model which produces high accuracy using flux and rejection values from experiments. Also, the membrane transport was used by the SHP model and found the effective pore radius of each heavy metals for both membranes. The model values show good correlation with experimental values of NF process for a wider range of concentration. We could conclude that AFC 30 and AFC 80 membranes can be used to remove heavy metals to some extent.

## References

AGBOOLA, O., MAREE, J., KOLESNIKOV, A., MBAYA, R., SADIKU, R. Theoretical performance of nanofiltration membranes for wastewater treatment. *Environmental Chemistry Letters*, 2015, 13, 37–47.

BAKER, R.W. Membrane Technology and Applications, 2nd edition, John Wiley & Sons Ltd, Chichester, United Kingdom, 2004.

BARAKAT, M. New trends in removing heavy metals from industrial wastewater. *Arabian Journal of Chemistry*, 2011, 4, 361–377.

BIAN, R., YAMAMOTO, K., WATANABE, Y. The effect of shear rate on controlling the concentration polarization and membrane fouling. *Desalination*, 2000, 131, 225–236.

BOURANENE, S., FIEVET, P., SZYMCZYK, A., EL-HADI SAMER, M., VODONNE, A. Influence of operating conditions on the rejection of cobalt and lead ions in aqueous solutions by a nanofiltration polyamide membrane. *Journal of Membrane Science*, 2008, 325, 150–157.

BOURANENE, S., FIEVET, P., SZYMCZYK, A. Investigating nanofiltration of multi-ionic solutions using the steric, electric and dielectric exclusion model. *Chemical Engineering Science*, 2009, 64, 3789–3798.

BOURANENE, S., FIEVET, P., SZYMCZYK, A., SAMER EL-HADI, M., VIODONNE, A. Influence of operating conditions on the rejection of cobalt and lead ions aqueous solutions by nanofiltration polyamide membrane. *Journal of Membrane Science*, 2008, 325, 150–157.

BOWEN, W.R., MOHAMMAD, A.W. Diafiltration by nanofiltration: prediction and optimization. *AIChE Journal*, 1998, 44, 1799–1812.

BOWEN, W.R., MOHAMMAD, A.W., HILAL, N. Characterization of nanofiltration membranes for predictive purposes—use of salts, uncharged solutes and atomic force microscopy. *Journal of Membrane Science*, 1997, 126, 91–105.

BOWEN, W.R., MUKHTAR, H. Characterisation and prediction of separation performance of nanofiltration membranes. *Journal of Membrane Science*, 1996, 112, 263–274.

BOWEN, W.R., WELFOOT, J.S. Modelling the performance of membrane nanofiltration—critical assessment and model development. *Chemical Engineering Science*, 2002, 57, 1121–1137.

CAVACO MORÃO, A.I., SZYMCZYK, A., FIEVET, P., BRITES ALVES, A.M. Modelling the separation by nanofiltration of a multi-ionic solution relevant to an industrial process, *Journal of Membrane Science*, 2008, 322, 320–330.

CHILDRESS, A.E., ELIMELECH, M. (2000) Relating nanofiltration membrane performance to membrane charge (Electro kinetic) characteristics, *Environmental Science & Technology*, 2000, 34, 3710–3716.

DECHADILOK, P., DEEN, W.M. Hindrance factors for diffusion and convection in pores. *Industrial & Engineering Chemistry Research*, 2006, 45, 6953–6959.

FU, F., WANG, Q. Removal of heavy metal ions from wastewaters: A review. *Journal of Environmental Management*, 2011, 92, 407–418.

GARCÍA –MARTIN, N., SILVA, V., CARMONA, F.J., PALACIO, L., HERNADEZ A., PRÁDANOS, P. Pore size analysis from retention of neutral solutes through nanofiltration membranes. The contribution of concentration-polarization. *Desalination*, 2014, 344, 1–11.

GEENS, J., DE WITTE, B., VAN DER BRUGGEN, B. Removal of API's (Active Pharmaceutical Ingredients) from organic solvents by nanofiltration. *Separation Science and Technology*, 2007, 42, 2435–2449.

GHERASIM, C.V., CUHORKA, J., MIKULÁŠEK, P. Analysis of lead (II) retention from single salt and binary aqueous solutions by a polyamide nanofiltration membrane: experimental results and modelling. *Journal of Membrane Science*, 2013, 436, 132–144.

GHERASIM, C.V., HANCKOVÁ, K., PALARČÍK, J., MIKULÁŠEK, P. Investigation of cobalt (II) retention from aqueous solutions by a polyamide nanofiltration membrane. *Journal of Membrane Science*, 2015, 490, 46–56.

GHERASIM, C.V., MIKULÁŠEK, P. Influence of operating variables on the removal of heavy metals ions from aqueous solution by nanofiltration. *Desalination*, 2014, 343, 67–74.

GHERASIM, C.V., MIKULÁŠEK, P., CHÝLKOVÁ J., KREJČOVÁ, A. Evaluation of structural and charge properties of polyamide nanofiltration membrane. *Scientific Papers of the University of Pardubice, Series A; Faculty of Chemical Technology*, 2014, 20, 343–352.

HOFFER, E., KEDEM, O. Hyperfiltration in charged membranes: The fixed charge model. *Desalination*, 1967, 2, 25–39.

HUANG, J.H., ZENG, G.M., ZHOU, C.F., LI, X., SHI, L.J., HE, S.B. Adsorption of surfactant micelles and $Cd^{2+}/Zn^{2+}$ in micellar-enhanced ultrafiltration. *Journal of Hazardous Materials*, 2010, 183, 287–293.

HUNG, D.C., NGUYEN, N.C., UAN, D.K., SON, L.H. Membrane processes and their potential applications for freshwater provision in Vietnam. *Vietnam Journal of Chemistry*, 2017, 55, 533–544.

LANTERI, Y., SZYMCZYK, A., FIEVET, P. Influence of steric, electric, and dielectric effects on membrane potential. *Langmuir*, 2008, 24, 7955–7962.

MALIK, M.A., HASHIM, M.A., NABI, F. Extraction of metal ions by ELM separation technology. *Journal of Dispersion Science and Technology*, 2012, 33, 346–356.

MEHDIPOUR, S., VATANPOUR, V., KARIMINIA, H-R. Influence of ion interaction on lead removal by a polyamide nanofiltration membrane, *Desalination*, 2015, 362, 84–92.

MIKULÁŠEK, P., CUHORKA, J. Removal of heavy metals from aqueous solutions by Nanofiltration. *Chemical Engineering Transactions*, 2016, 47, 379–384.

MOHAMMAD A.W., TEOW Y.H., ANG W.L., CHUNG Y.T., OATLEY-RADCLIFFE D.L., HILAL N. Nanofiltration membrane review: Recent advances and future prospects. *Desalination*, 2015, 356, 226–254.

MULDER, M. Basic Principles of Membrane Technology, 2nd ed., Kluwer Academic Publishers, 1997.

MURTHY, Z. V. P., CHAUDHARI, L. B. Application of nanofiltration for the rejection of nickel ions from aqueous solutions and estimation of membrane transport parameters. *Journal of Hazardous Materials*, 2008, 160, 70–77.

NAIR, R.R., PROTASOVA, E., STRAND, S., BILSTAD, T. Implementation of Spiegler–Kedem and Steric Hindrance Pore Models for analysing nanofiltration membrane performance for smart water production. *Membranes (Basel)*, 2018, 8, 1–16.

NAKAO, S., KIMURA, S. Models of membrane transport phenomena and their applications for ultrafiltration data. *Journal of Chemical Engineering of Japan*, 1982, 15, 200–205.

O'CONNELL, D.W., BIRKINSHAW, C., O'DWYER, T.F. Heavy metal adsorbents prepared from modification of cellulose: a review. *Bioresource Technology*, 2008, 15, 6709–6724.

QADIR, D., MUKHTAR, H.B., KEONG, L.K. Rejection of divalent ions in commercial tubular membranes: Effect of feed concentration and anion type. *Sustainable Environmental Research*, 2017, 27, 103–106.

SCHAEP J., VANDECASTEELE, C., MOHAMMAD A. W., BOWEN W. R. Analysis of the salt retention of nanofiltration membranes using the Donnan-steric partitioning pore model. *Separation Science and Technology*, 1999, 34, 3009–3030.

SEIDEL, A., ELIMELECH, M. Coupling between chemical and physical interactions in natural organic matter (NOM) fouling of nanofiltration membranes: Implications for fouling control, *Journal of Membrane Science*, 2002, 203, 245–255.

SPIEGLER, K.S., KEDEM, O. Thermodynamics of hyperfiltration (reverse osmosis): Criteria for efficient membranes. *Desalination*, 1966, 1, 311–326.

SZYMCZYK, A., FATIN-ROUGE, N., FIEVET, P. Tangential streaming potential as a tool in modelling of ion transport through nanoporous membranes. *Journal of Colloid and Interface Science*. 2007, 309, 245–252.

TCHOUNWOU, P.B., YEDJOU, C.G., PATLOLLA, A.K., SUTTON, D.J. Heavy metals toxicity and the environment. *National Institute of Health*, 2012, 101, 140–162.

VAN DER BRUGGEN, B., VANDECASTEELE, C., VAN GESTEL, T., DOYEN, W., LEYSEN, R. A review of pressure-driven membrane processes in wastewater treatment and drinking water production. *Environmental Progress*, 2003, 22, 46–56.

VANÝSEK, P. Ionic conductivity and diffusion at infinite dilution, in: D.R. Linde (Ed.), CRC Handbook of Chemistry and Physics, 84th ed., CRC Press, Boca Raton, 2005.

WALLACE, E., CUHORKA, J., MIKULÁŠEK, P. Investigation of the structural and charge properties of a polyamide nanofiltration membrane, *Scientific Papers of the University of Pardubice, Series A; Faculty of Chemical Technology*, 2017, 23, 225–243.

WANG X.L., FANG Y.Y., TU C.H., VAN DER BRUGGEN, B. Modelling of the separation performance and electrokinetic properties of nanofiltration membranes. *International Reviews in Physical Chemistry*, 2012, 31,111–130.

WANG X.L., TSURU T., TOGOH M., NAKAO S., KIMURA S. Evaluation of pore structure and electrical properties of nanofiltration. *Journal of Chemical Engineering of Japan*, 1995, 28, 186–192.

WEI, X., KONG, X., WANG, S., XIANG, H., WANG, J., CHEN, J. Removal of heavy metals from electroplating wastewater by thin–film composite nanofiltration hollow–fiber membranes. *Industrial & Engineering Chemistry Research*, 2013, 52, 17583–17590.

ZHAO, F.Y., JI, Y.L., WENG, X.D., MI, Y.F., YE, C.C., AN, Q.F., GAO, C.J. High-flux positively charged nanocomposite nanofiltration membranes filled with poly(dopamine) modified multiwall carbon nanotubes. *ACS Applied Materials & Interfaces*, 2016, 8, 6693–6700.

ZHAO, K., LI, Y. Dielectric characterization of a nanofiltration membrane in electrolyte solutions: Its double–layer structure and ion permeation. *Journal of Physical Chemistry*, 2006, 110, 2755–2763.

## List of Student' Published Works

WALLACE, E., CUHORKA, J., MIKULÁŠEK, P. Investigation of the structural and charge properties of a polyamide nanofiltration membrane, *Scientific Papers of the University of Pardubice, Series A; Faculty of Chemical Technology,* 2017, 23, 225–243.

WALLACE, E., CUHORKA, J., MIKULÁŠEK, P. Interpretation of structural and electrical properties of a polyamide nanofiltration membrane, *9th International conference on nanomaterials - Research & Application* (NANOCON 2017), 871–876, Published: 2018 (Proceedings Paper).

WALLACE, E., CUHORKA, J., MIKULÁŠEK, P. Characterization of nanofiltration membrane and its application for the separation of heavy metals from wastewater. *Waste Forum*, 2018, 2, 314–325.

CUHORKA, J., WALLACE, E., MIKULÁŠEK, P. Removal of micropollutants from water by commercially available nanofiltration membranes. *Science of The Total Environment,* 2020, 720, 137474.

### Proceedings

WALLACE, E., CUHORKA J., MIKULÁŠEK, P. Investigation of structural properties of a polyamide nanofiltration membrane. In Membranes and membrane processes. Česká Lípa: Česká membránová platforma (CZEMP), 2016, s. 26. ISBN 978-80-9045-8-0.

WALLACE, E., CUHORKA, J., MIKULÁŠEK, P. Influence of operating parameters on the rejection of zinc ions from aqueous solution by a nanofiltration polyamide membrane, SSCHE, Demänovská dolina, 2017, s. 6–15, ISBN 978-80-89597-58-1.

WALLACE, E., CUHORKA, J., MIKULÁŠEK, P. Interpretation of structural and Electrical properties of a Polyamide Nanofiltration Membrane, NANOCON, Brno, 2017, s. 157. IBSN 978-80-87294-78-9.

WALLACE, E., CUHORKA, J., MIKULÁŠEK, P. Investigation of zinc (II) retention from aqueous solution by a polyamide nanofiltration membrane. Experimental results and modelling. MEMPUR, Pardubice, 2017, s. 83, ISBN 978-80-904517-9-7.

WALLACE, E., CUHORKA, J., MIKULÁŠEK, P. Characterization of nanofiltration and its practical application use for the separation of zinc from waste wastewater. SSCHE, Tatranské Matliare, 2018, s. 314, ISBN 978-80-89597-89-5.

WALLACE, E., CUHORKA, J., MIKULÁŠEK, P. Characterization of nanofiltration membrane and its application for the separation of heavy metals from wastewater. MELPRO, Prague, 2018, s. 128, ISBN 978-80-906831-2-9.